

Supplemental Information for

NiFeCo-based Catalysts in High Current Zero-Gap

Anion Exchange Membrane Water Electrolyzers

B. Milenia Rojas Mendoza^{1,2}, Ryan T. Hannagan^{1,2,3}, Sofia Kimuyu¹, Colin F. Crago^{1,2}, Alfred Vargas^{1,2}, Ashton M. Aleman^{1,2}, Johanna Schröder⁴, Daniela H. Marin^{1,2}, Isabela Rios Amador^{1,2}, Jaehyuk Shim^{1,2}, Adam C. Nielander², Michaela Burke Stevens^{2}, Thomas F. Jaramillo^{1,2*}*

¹Department of Chemical Engineering, Stanford University, 443 Via Ortega, Stanford, CA 94305, United States of America

²SUNCAT Center for Interface Science and Catalysis, SLAC National Accelerator Laboratory, 2575 Sand Hill Road, Menlo Park, CA 94025, United States of America

³Department of Chemical Sciences, Bridgewater State University, Bridgewater, MA 02325

⁴Institute for Chemical Technology and Polymer Chemistry (ITCP), Karlsruhe Institute of Technology (KIT), Engesserstrabe 18, 76131, Karlsruhe, Germany.

Corresponding Authors

*Email: mburkes@slac.stanford.edu, jaramillo@stanford.edu

Table of Contents

Material Characterization3

Figure S1: XPS depth profile of bimetallic and trimetallic thin films.....3
 Figure S2. XRD patterns of PVD-deposited thin-film anode catalysts and reference standards. ...4
 Figure S3. SEM images and EDS elemental maps of catalyst-coated PTLs and controls.....5
 Figure S4. Electrochemical Schematic6
Additional Data 7
 Figure S5. Pre- and post-24 h stability polarization curves in DI water-fed AEMWEs.....7
 Figure S6. Quantified metal dissolution from anode catalyst layers after 24 h at 1 A cm⁻² in DI water.8
 Figure S7. XPS of ionomer and catalyst surfaces before and after 24 h stability testing.....9
 Figure S8. Raw galvanostatic electrochemical impedance spectroscopy (GEIS) Nyquist plots for each anode catalyst at 1 A cm⁻².10

Material Characterization

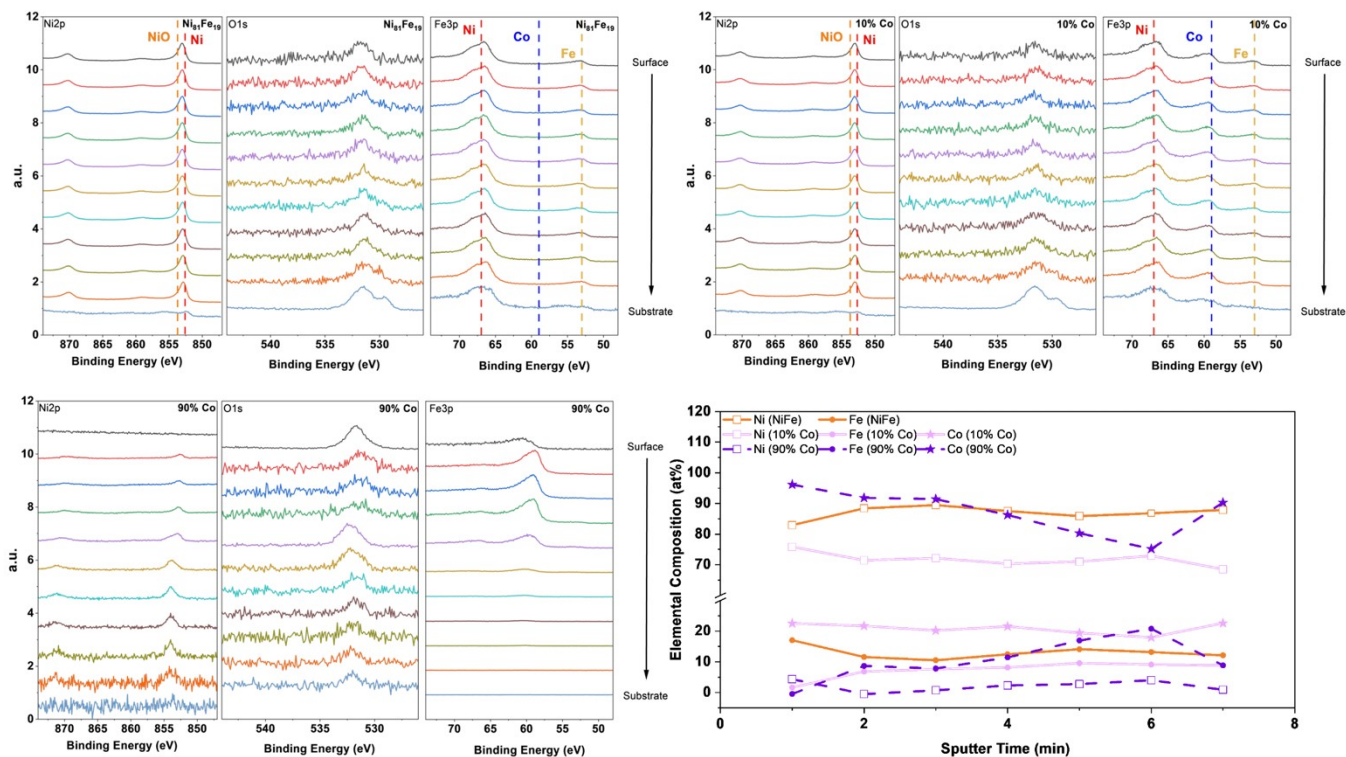


Figure S1: XPS depth profile of bimetallic and trimetallic thin films

Panels (a–c) show stacked spectra of the Ni 2p (left), O 1s (center) and Fe 3p (right) regions after successive Ar⁺ sputter intervals (surface at top, substrate at bottom) for: a) Ni₈₁Fe₁₉, b) (Ni₈₁Fe₁₉)₉₀Co₁₀, and c) (Ni₈₁Fe₁₉)₁₀Co₉₀. Dashed red lines mark the Ni⁰/Ni²⁺ peaks in Ni 2p, dashed yellow lines the O 1s oxide peak, and dashed blue (Fe 3p) and orange (Fe 3p satellite) lines the iron signals. d) Quantified at.% of Ni, Fe and Co extracted from the Fe 3p and Ni 2p peaks as a function of sputter time for all three alloys, demonstrating that each film maintains its target composition ($\sim\pm 10\%$) throughout the ~ 100 nm thickness.

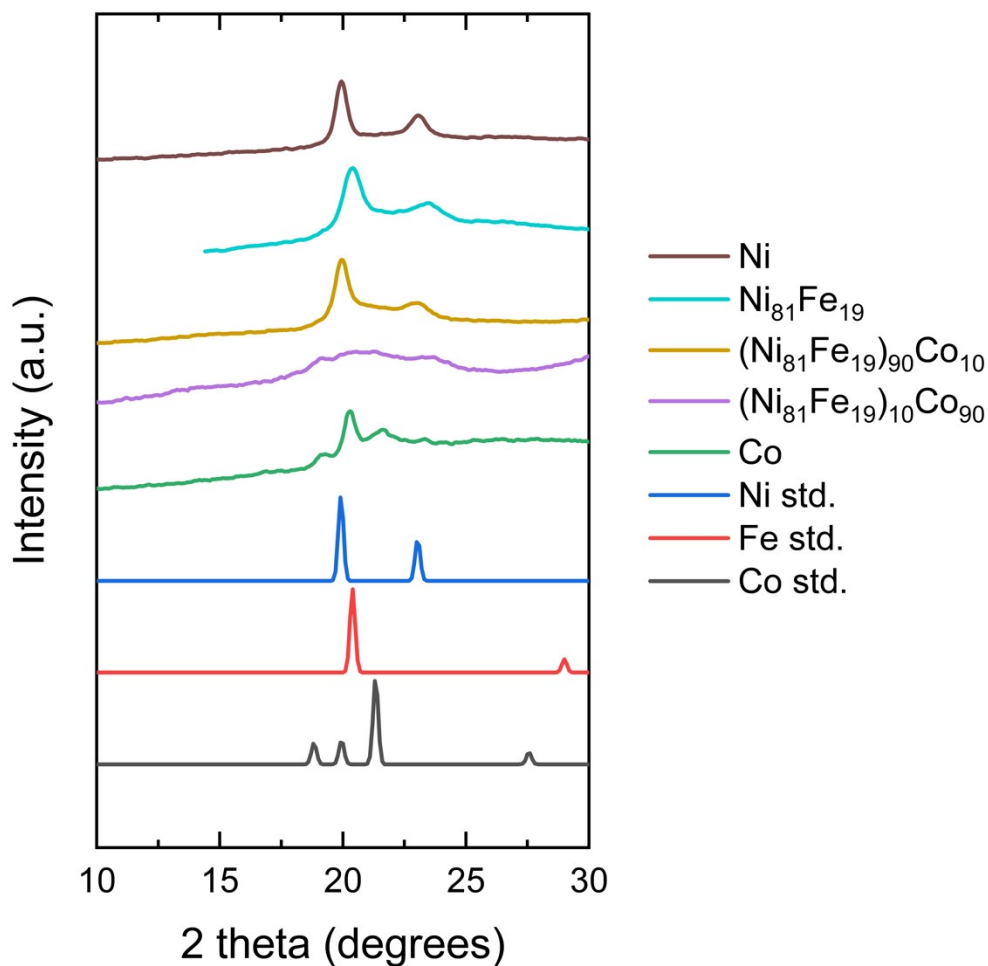


Figure S2. XRD patterns of PVD-deposited thin-film anode catalysts and reference standards.

Diffraction traces for 100 nm Ni (brown), Ni₈₁Fe₁₉ (cyan), (Ni₈₁Fe₁₉)₉₀Co₁₀ (gold), (Ni₈₁Fe₁₉)₁₀Co₉₀ (purple), and 100 nm Co (green) alongside ICSD metallic standards for Ni (blue, ICSD 125671), Fe (red, ICSD 14754), and Co (grey, ICSD 36677). All compositions exhibit

primarily FCC metal peaks: Ni-rich films align with the Ni reference, Co-rich films align with Co, and intermediate alloys display peak shifts and broadening consistent with alloy formation.

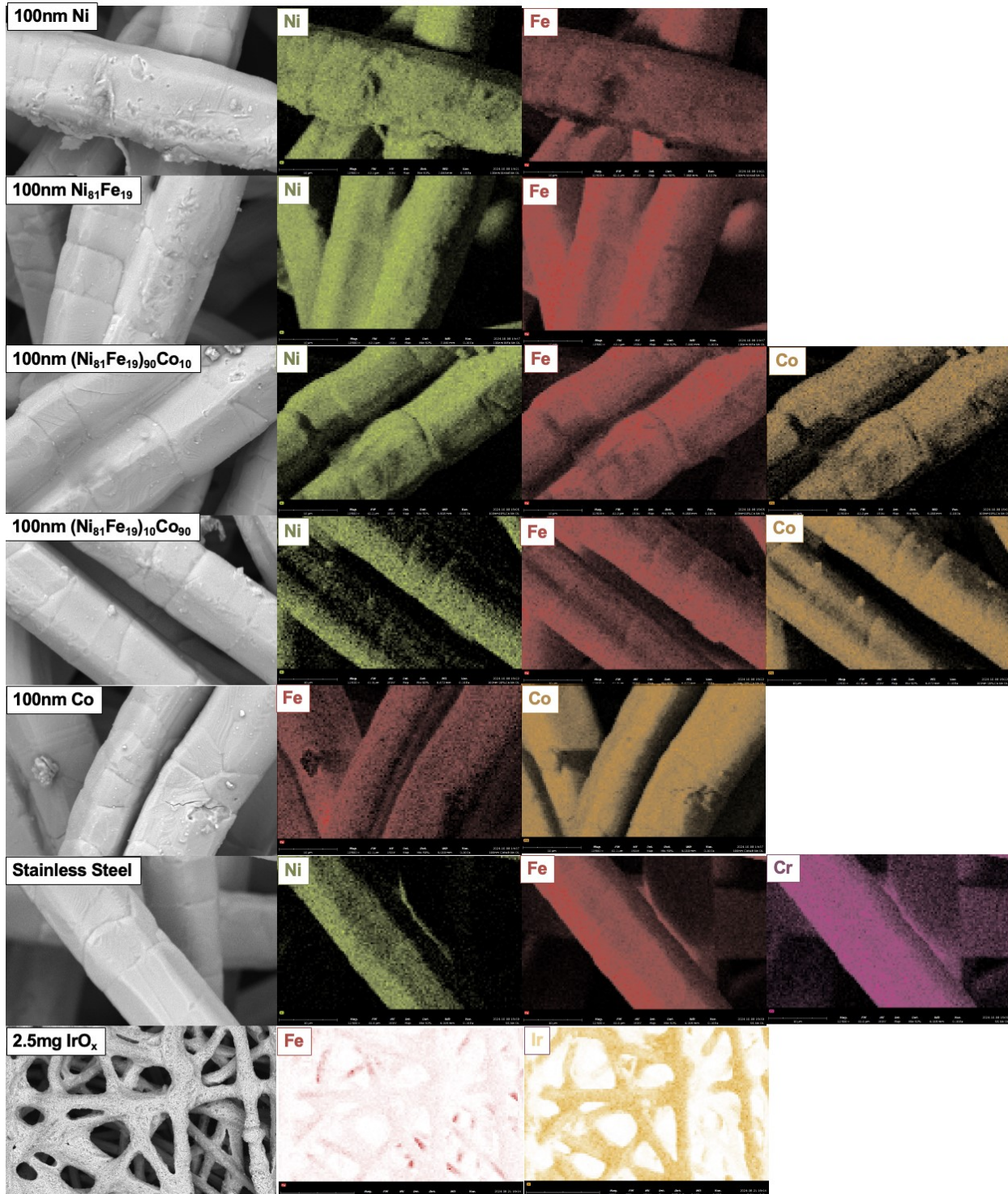


Figure S3. SEM images and EDS elemental maps of catalyst-coated PTLs and controls. a–g, Secondary-electron SEM (left) and corresponding EDS maps (Ni in green, Fe in red, Co in gold, Cr in magenta or Ir in yellow) for (a) 100 nm Ni, (b) 100 nm Ni₈₁Fe₁₉, (c) 100 nm (Ni₈₁Fe₁₉)₁₀Co₉₀, (d) 100 nm (Ni₈₁Fe₁₉)₉₀Co₁₀, (e) 100 nm Co, (f) bare stainless-steel PTL, and (g) 2.5 mg cm⁻² IrO_x nanoparticles. All PVD-deposited films uniformly coat the porous steel fibers with homogeneous elemental distribution, whereas the uncoated PTL exhibits only Cr and Fe signals and the IrO_x sample displays discrete Ir-rich agglomerates.

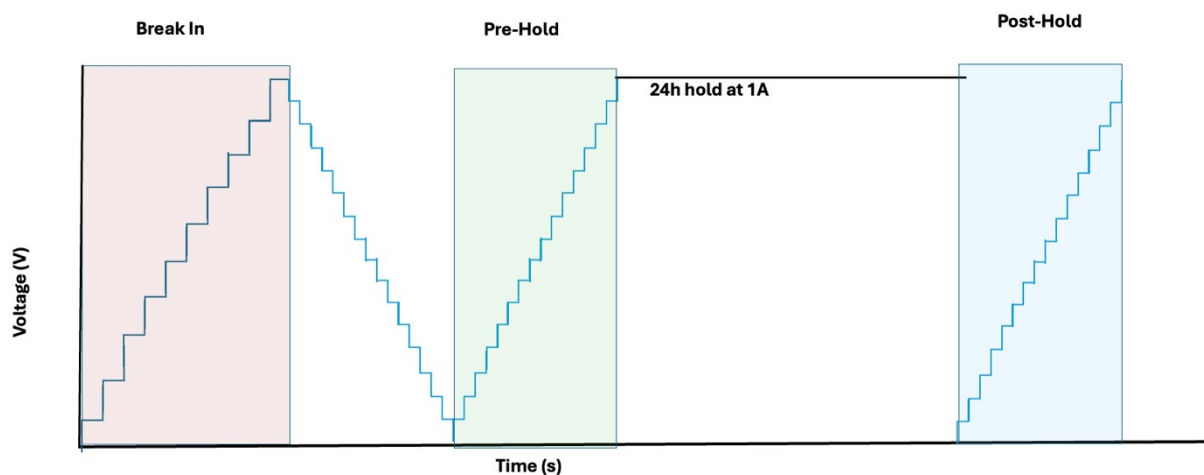


Figure S4. Electrochemical Schematic

An electrochemical sequence was applied at 50 °C with 60 mL min⁻¹ feed: (i) Break-in (red shading), a staircase polarization from 0 to 1 A cm⁻² in 100 mA cm⁻² increments followed immediately by a reverse staircase back to 50 mA cm⁻²; (ii) Pre-hold polarization (green shading), a repeat staircase from 50 mA to 1 A cm⁻² to establish the baseline polarization curve; (iii) 24 h galvanostatic hold at 1 A cm⁻² (black line), after which (iv) Post-hold polarization (blue shading) repeats the staircase from 50 mA to 1 A cm⁻² to quantify voltage change over time and post-stability performance. Continuous voltage measurements were recorded at each current step.

Additional Data

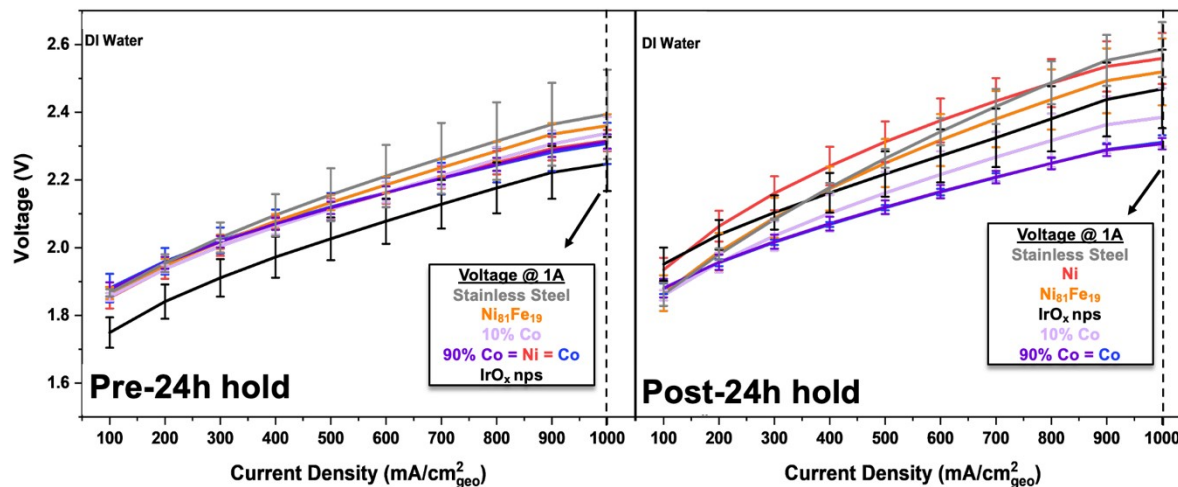


Figure S5. Pre- and post-24 h stability polarization curves in DI water-fed AEMWEs.

Average voltage current density relationships ($100\text{--}1000\text{ mA cm}^{-2}\text{_{geo}}$, $n = 3$) are shown for stainless-steel PTL (grey), Ni (red), $\text{Ni}_{81}\text{Fe}_{19}$ (orange), IrO_x nanoparticles (black), 10 % Co (purple) and 90 % Co (blue) thin-film anodes. Left: “Pre-24 h hold” polarization curves recorded immediately after the break-in protocol. Right: “Post-24 h hold” curves recorded following a 24 h galvanostatic hold at 1 A cm^{-2} . The dashed vertical line at $1000\text{ mA cm}^{-2}\text{_{geo}}$ denotes the 1 A cm^{-2} endpoint; inset boxes list the corresponding voltages at this current density for each catalyst.

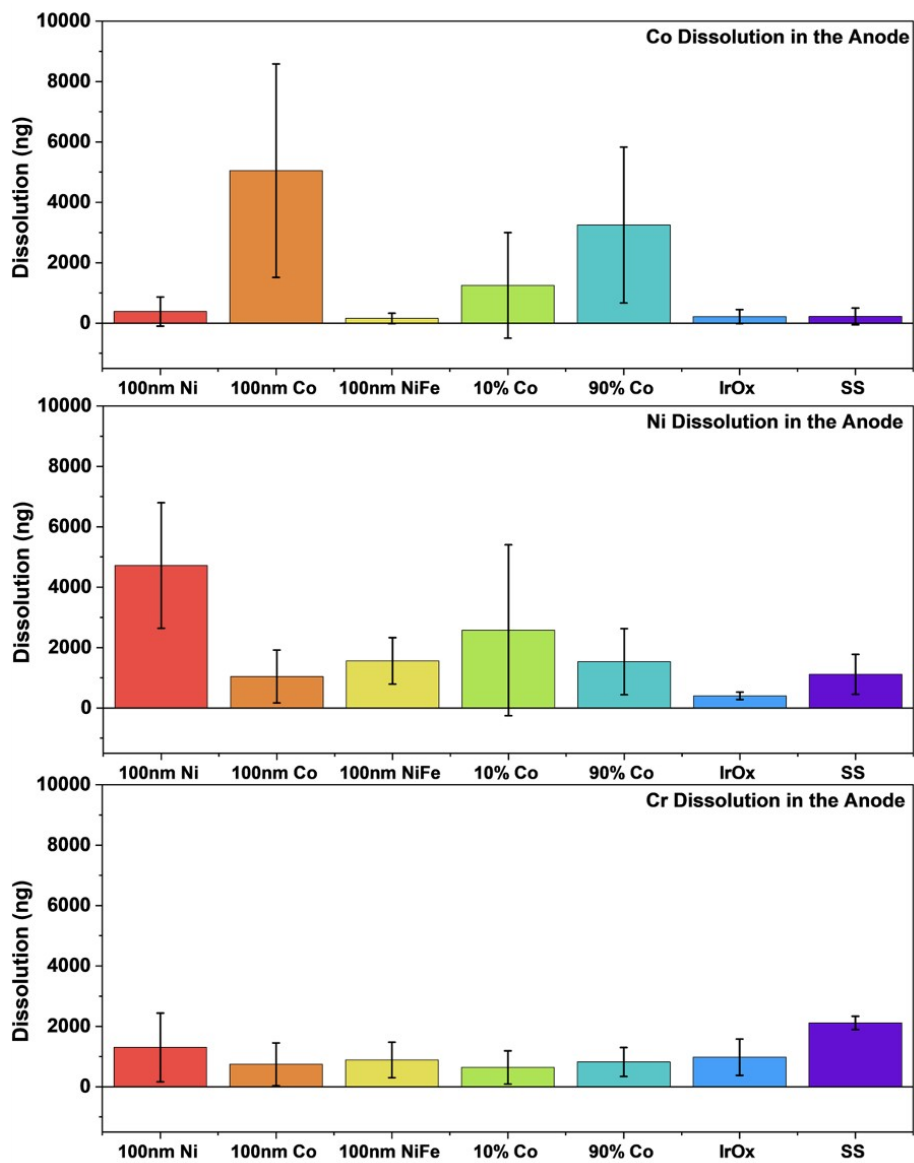


Figure S6. Quantified metal dissolution from anode catalyst layers after 24 h at 1 A cm^{-2} in DI water.

Top panel shows Co, middle panel Ni, and bottom panel Cr dissolved (ng) from 100 nm Ni, 100 nm Co, 100 nm Ni₈₁Fe₁₉, 10 % Co, 90 % Co, 2.5 mg cm⁻² IrO_x, and bare stainless-steel (SS) PTLs. Bars represent the mean \pm SD of three independent MEAs, with the stainless-steel control blank (\sim 1 ppb Ni threshold) subtracted.

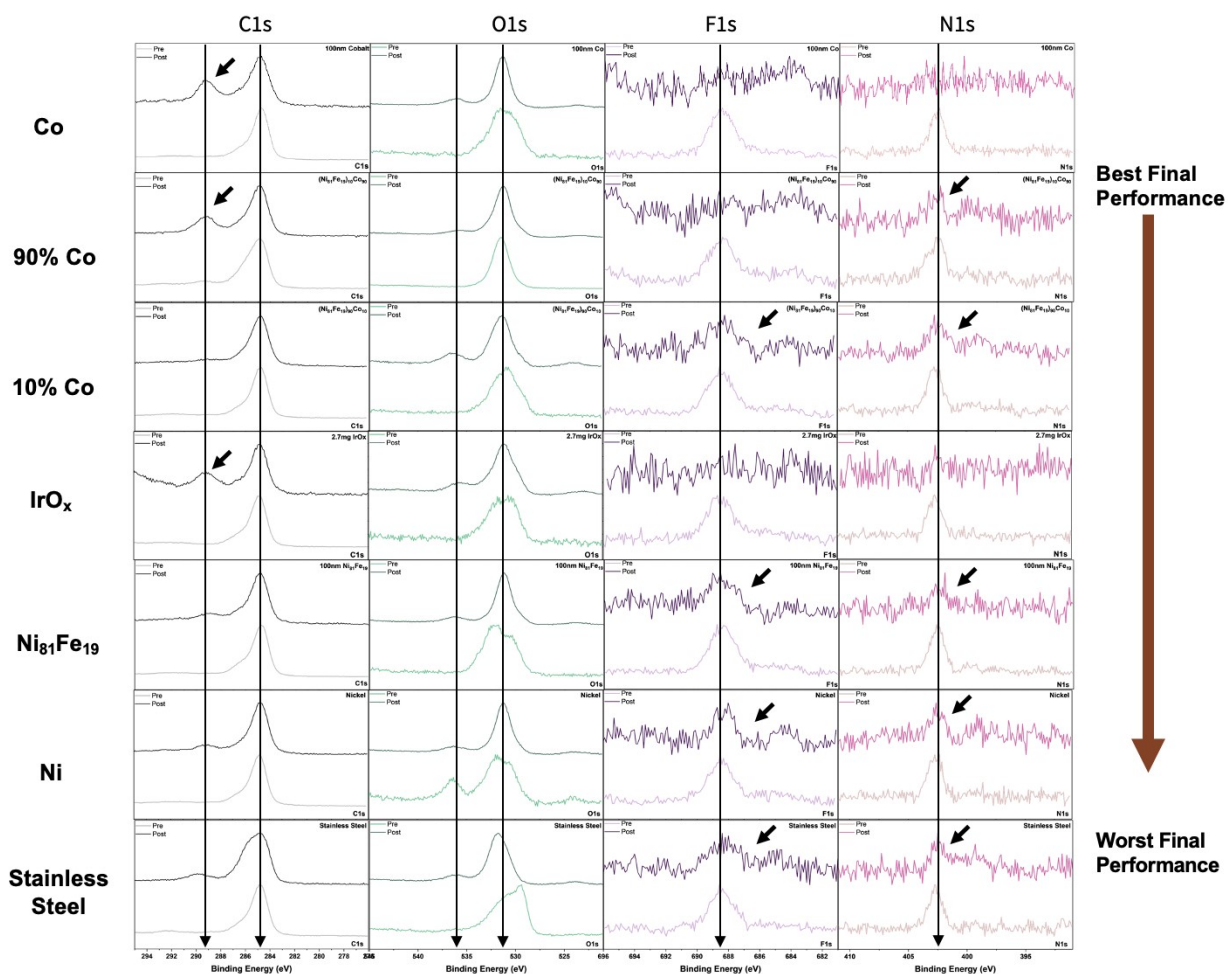


Figure S7. XPS of ionomer and catalyst surfaces before and after 24 h stability testing.

Rows, from top to bottom, correspond to the anode catalysts ordered by decreasing final performance (best at top: Co, 90 % Co, 10 % Co; mid: IrO_x, Ni₈₁Fe₁₉; worst at bottom: Ni, stainless-steel PTL). Columns show the C 1s (left), O 1s, F 1s and N 1s (right) regions, with each spectrum overlaid “Pre” (light line) and “Post” (darker line) the 24 h hold at 1 A cm⁻². Vertical guide lines mark the principal binding energies: C=C (~284.8 eV), C–O (~286.5 eV), C=O (~288.5 eV), O 1s oxide (~531.5 eV), F 1s (~689 eV) and N 1s (~399 eV). Black arrows highlight the growth of the C=O shoulder in C 1s and the emergence or attenuation of F 1s and N 1s peaks from ionomer degradation.

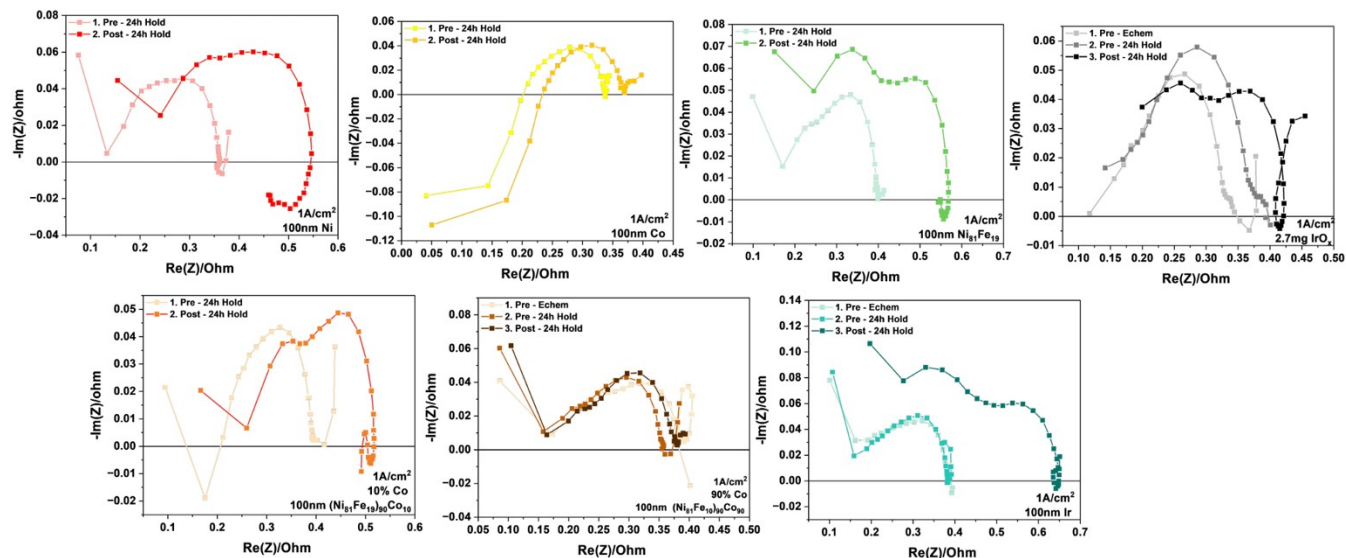


Figure S8. Raw galvanostatic electrochemical impedance spectroscopy (GEIS) Nyquist plots for each anode catalyst at 1 A cm^{-2} .

Panels show $-\text{Im}(Z)$ vs $\text{Re}(Z)$ for (a) 100 nm Ni, (b) 100 nm Co, (c) 100 nm $\text{Ni}_{81}\text{Fe}_{19}$, (d) 2.5 mg cm^{-2} IrO_x nanoparticles, (e) 100 nm $(\text{Ni}_{81}\text{Fe}_{19})_{10}\text{Co}_{90}$, (f) 100 nm $(\text{Ni}_{81}\text{Fe}_{19})_{90}\text{Co}_{10}$ and (g) 100 nm Ir (see colour legend). Light markers correspond to data recorded immediately before the 24 h stability hold (“Pre-24 h”), and dark markers to data recorded immediately after (“Post-24 h”); panels (c) and (d) additionally include the initial “Pre-Echem” response (grey). The decrease in semicircle diameter from light to dark traces for Co-rich alloys indicates a smaller increase in charge-transfer resistance during the 24 h hold compared to Ni-rich films.